Flexural Wave Propagation in Slowly Varying Random Waveguides Using a Finite Element Approach

A T Fabro[1], N S Ferguson[2], B R Mace[3]

[1] Department of Mechanical Engineering, University of Brasília, 70910-900, Brasília-DF, Brazil
[2] ISVR, University of Southampton, Highfield Campus, SO17 1BJ, UK
[3] Department of Mechanical Engineering, University of Auckland, Private Bag 92019, Auckland 1142, New Zealand

Corresponding's author email: fabro@unb.br

Abstract. This work investigates structural wave propagation in waveguides with randomly varying properties along the axis of propagation, specifically when the properties vary slowly enough such that there is negligible backscattering. Wave-based methods are typically applied to homogeneous waveguides but the WKB (after Wentzel, Kramers and Brillouin) approximation can be used to find a suitable generalisation of the wave solution in terms of the change of phase and amplitude, but is restricted to analytical solutions. A wave and finite element (WFE) approach is proposed to extend the applicability of the WKB method to cases where no analytical solution is available. The wavenumber is expressed as a function of the position along the waveguide and a Gauss-Legendre quadrature scheme is used to obtain the phase change while the wave amplitude is calculated using conservation of power. The WFE method is used to evaluate the wavenumbers at each integration point. The flexural vibration example is considered with random field proprieties being expressed by a Karhunen-Loeve expansion. Results are compared to a standard FE approach and to the WKB analytical solution. They show good agreement and require only a few WFE evaluations, providing a suitable framework for spatially correlated randomness in waveguides.

1. Introduction

Wave-based methods commonly assume that waveguide properties are homogeneous in the direction of the travelling wave, limiting the application of such approaches. This assumption arises mainly because analytical solutions for non-homogeneous waveguides are only possible for very particular cases, for example acoustic horns, ducts, rods and beams, e.g. [1–4]. Moreover, randomly varying material and geometric properties along the axis of propagation play a significant role in the so-called mid-frequency region.

The WFE approach is a wave based method that is used to predict the wavenumbers and wave modes of a waveguide from a FE model, by post processing the mass and stiffness matrices, typically found using a FE package. This is particularly useful when no analytical solution is available and conventional FE models became excessively large. This method has been applied to a number of cases in structural dynamics including free and forced vibration [5–13]. Even though it can be used to model non-uniform cross-sections, this approach is however limited to homogeneous or piecewise constant waveguides in the direction of the travelling wave.

The classical WKB approximation is a method for finding suitable modifications of plane-wave solutions for non-homogeneous waveguides [14]. Named after Wentzel, Kramers and Brillouin, it was initially developed for solving the Schrödinger equation in quantum mechanics. The formulation assumes that the waveguide properties vary slowly enough such that there are no or negligible reflections due to these local changes, even if the net change is large, and can be extended to include spatially correlated random variability [15]. It maintains the wave-like interpretation of non-uniform waveguides, but it is restricted to available analytical solutions.

In this work, a Wave and Finite Element (WFE) approach is proposed to extend the applicability of the WKB method to cases where no analytical solution is available. The wave proprieties are calculated using the WFE approach and they are expressed as a function of the position along the waveguide. A brief review of the method is presented. The phase change is calculated using a Gauss-Legendre quadrature scheme for numerical integration of the local wavenumber. The WFE method is used to evaluate the wavenumbers at each integration point, and these are kept to a minimum to reduce computation cost while being able to capture the non-homogeneity to a given accuracy. The wave amplitude change is calculated using conservation of power.

The numerical example of a straight beam with propagating and evanescent wave modes is considered with non-uniform material and geometrical properties. Random field properties are expressed in terms of a Karhunen-Loeve (KL) expansion, and an analytical solution for a specific family of non-uniform waveguides [4] is presented for comparison. The forced response to a point excitation is calculated and results are compared to a standard Finite Element (FE) approach and to the WKB analytical solution. Results show good agreement and require only a few WFE evaluations, providing a suitable framework to account for spatially correlated randomness in waveguides.

2. The WKB approximation

The WKB formulation has been applied in many fields of engineering, including, acoustics [16,17] and structural dynamics [14,15,18]. However, the WKB approximation breaks down if the properties change rapidly or when the travelling wave reaches a local cut-off section where the wave mode ceases to propagate. This transition, also known as a turning point, leads to an internal reflection, breaking down the main assumption in the theory, requiring a different approximation for certain frequency bands (e.g. [19]).

Assuming a time harmonic solution, $u(x,t) = U(x)\, e^{-i\omega t}$, it is possible to define a local wavenumber $k(x)$. Thus, the *eikonal* function $S(x) = \ln \widetilde{U}(x) + i\theta(x)$ is introduced, in order to find wave solutions of the kind [20]

$$U(x) = e^{S(x)} = \widetilde{U}(x) e^{\pm i\theta(x)}. \tag{1}$$

It is possible to define positive $\mathbf{b}^+ = \mathbf{\Lambda}^+(x_a, x_b)\mathbf{a}^+$ and negative going $\mathbf{b}^- = \mathbf{\Lambda}^-(x_a, x_b)\mathbf{a}^-$ propagation matrices for a wave travelling between x_a and x_b. Forced response can be considered as in Fig. 1, where the wave amplitudes are given at the excitation point by

$$\mathbf{c}^+ = \mathbf{e}^+ + \mathbf{b}^+ \text{ and } \mathbf{b}^- = \mathbf{e}^- + \mathbf{c}^-, \tag{2}$$

where $\mathbf{e}^+$ and $\mathbf{e}^-$ are the amplitude of the waves directly generated from the excitation that can be calculated from equilibrium and continuity conditions. Wave amplitudes at the boundaries are related by the reflection matrices as $\mathbf{a}^+ = \mathbf{\Gamma}_L \mathbf{a}^-$ and $\mathbf{d}^- = \mathbf{\Gamma}_R \mathbf{d}^+$. The traveling waves amplitudes are related by the propagating matrices as $\mathbf{b}^+ = \mathbf{\Lambda}^+(0, L_e)\mathbf{a}^+$, $\mathbf{d}^+ = \mathbf{\Lambda}^+(L_e, L)\mathbf{c}^+$, $\mathbf{a}^- = \mathbf{\Lambda}^-(L_e, 0)\mathbf{b}^-$, $\mathbf{c}^- = \mathbf{\Lambda}^-(L, L_e)\mathbf{d}^-$, $\mathbf{h}^+ = \mathbf{\Lambda}^+(L_e, L_r)\mathbf{c}^+$ and $\mathbf{h}^- = \mathbf{\Lambda}^-(L, L_r)\mathbf{d}^-$.

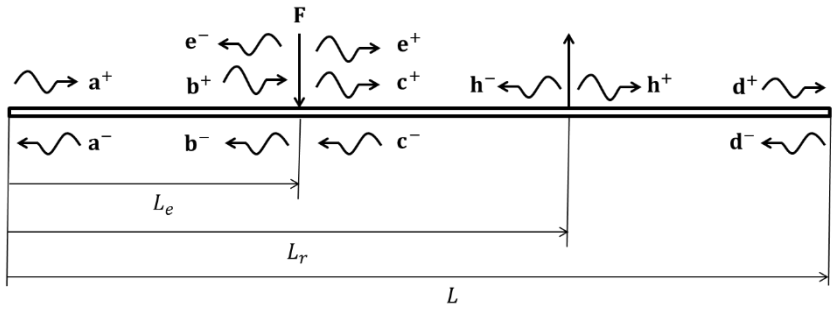

Figure 1. Point excitation and wave amplitudes on a waveguide with slowly varying properties.

These relations can be used to find

$$\mathbf{c}^+ = [\mathbf{I} - \boldsymbol{\Lambda}^+(0, L_e)\boldsymbol{\Gamma}_L\boldsymbol{\Lambda}^-(0, L)\boldsymbol{\Gamma}_R\boldsymbol{\Lambda}^+(L_e, L)]^{-1}[\mathbf{e}^+ + \boldsymbol{\Lambda}^+(0, L_e)\boldsymbol{\Gamma}_L\boldsymbol{\Lambda}^-(0, L_e)\mathbf{e}^-], \tag{3}$$

$$\mathbf{c}^- = \boldsymbol{\Lambda}^-(L, L_e)\boldsymbol{\Gamma}_R\boldsymbol{\Lambda}^+(L_e, L)\mathbf{c}^+, \tag{4}$$

from which the input mobility can be calculated. The same rationale can be used to calculate the response at any point in the waveguide from the wave amplitudes $\mathbf{h}^+$ and $\mathbf{h}^-$.

3. The wave and finite element approximation

In this section, a brief review of the WFE approach is presented for one-dimensional waveguides. A section of the waveguide of axial length Δ is cut from the structure and, assuming harmonic motion, its dynamic stiffness matrix $\widetilde{\mathbf{D}} = \mathbf{K} + i\omega\mathbf{C} - \omega^2\mathbf{M}$ can be obtained from a conventional FE analysis, such that $\widetilde{\mathbf{D}}\mathbf{q} = \mathbf{f}$, where $\mathbf{K}$, $\mathbf{C}$ and $\mathbf{M}$ are, respectively, the stiffness, damping and mass matrices, $\mathbf{q}$ is the vector of nodal degrees of freedom and $\mathbf{f}$ is the vector of nodal forces. The dynamic stiffness matrix $\widetilde{\mathbf{D}}$ can be condensed to eliminate the interior degrees of freedom, leading to the matrix $\mathbf{D}$ that can be partitioned as

$$\begin{bmatrix}\mathbf{D}_{LL} & \mathbf{D}_{LR}\\ \mathbf{D}_{RL} & \mathbf{D}_{RR}\end{bmatrix}\begin{bmatrix}\mathbf{q}_L\\ \mathbf{q}_R\end{bmatrix} = \begin{bmatrix}\mathbf{f}_L\\ \mathbf{f}_R\end{bmatrix}, \tag{5}$$

associating the degrees of freedom and nodal forces on the left (L) and the right (R) cross-section [6]. For a wave freely propagating along the waveguide, a propagation constant relates displacements and forces from the left and right side of the section, i.e. $\mathbf{q}_R^s = \lambda\mathbf{q}_L^s$ and $\mathbf{f}_R^s = -\lambda\mathbf{f}_L^s$. Moreover, from continuity of displacements and equilibrium of forces between sections s and $(s+1)$ it follows that $\mathbf{q}_L^{s+1} = \mathbf{q}_R^s$ and $\mathbf{f}_L^{s+1} = -\mathbf{f}_R^s$. Then, a transfer matrix can be defined such that

$$\begin{bmatrix}\mathbf{q}_L^{s+1}\\ \mathbf{f}_L^{s+1}\end{bmatrix} = \mathbf{T}\begin{bmatrix}\mathbf{q}_L^{s}\\ \mathbf{f}_L^{s}\end{bmatrix}, \tag{6}$$

where

$$\mathbf{T} = \begin{bmatrix}-\mathbf{D}_{LR}^{-1}\mathbf{D}_{LL} & \mathbf{D}_{LR}^{-1}\\ -\mathbf{D}_{RL} + -\mathbf{D}_{RR}\mathbf{D}_{LR}^{-1}\mathbf{D}_{LL} & -\mathbf{D}_{RR}\mathbf{D}_{LR}^{-1}\end{bmatrix}. \tag{7}$$

The eigenvalues/eigenvectors of the transfer matrix are separated in two sets of n positive-going λ_j and $\boldsymbol{\phi}_j^+$ and n negative-going $1/\lambda_j$ and $\boldsymbol{\phi}_j^-$ wave types and the j^{th} eigenvalue is written as $\lambda_j =$

$\exp(-ik_j\Delta)$. The eigenvectors can be rearranged such that $\boldsymbol{\phi}^+ = \begin{bmatrix}\boldsymbol{\phi}_q^+ \\ \boldsymbol{\phi}_f^+\end{bmatrix}$ and $\boldsymbol{\phi}^- = \begin{bmatrix}\boldsymbol{\phi}_q^- \\ \boldsymbol{\phi}_f^-\end{bmatrix}$ and then are used for a linear transformation of the displacement and force from the wave domain to the physical domain

$$\mathbf{q} = \boldsymbol{\phi}_q^+\mathbf{a}^+ + \boldsymbol{\phi}_q^-\mathbf{a}^- \text{ and } \mathbf{f} = \boldsymbol{\phi}_f^+\mathbf{a}^+ + \boldsymbol{\phi}_f^-\mathbf{a}^-, \tag{8}$$

where $\mathbf{a}^+$ and $\mathbf{a}^-$ are respectively positive-going and negative-going wave amplitudes. Any boundary condition can written as $\mathbf{Af} + \mathbf{Bq} = \mathbf{0}$, then the reflection matrices are given by [4,10]

$$\boldsymbol{\Gamma}_L = -\left(\mathbf{A}\boldsymbol{\phi}_{\mathrm{f}}^+ + \mathbf{B}\boldsymbol{\phi}_{\mathrm{q}}^+\right)^{-1}\left(\mathbf{A}\boldsymbol{\phi}_{\mathrm{f}}^- + \mathbf{B}\boldsymbol{\phi}_{\mathrm{q}}^-\right) \text{ and } \boldsymbol{\Gamma}_R = -\left(\mathbf{A}\boldsymbol{\phi}_{\mathrm{f}}^- + \mathbf{B}\boldsymbol{\phi}_{\mathrm{q}}^-\right)^{-1}\left(\mathbf{A}\boldsymbol{\phi}_{\mathrm{f}}^+ + \mathbf{B}\boldsymbol{\phi}_{\mathrm{q}}^+\right). \tag{9}$$

The amplitudes of the positive and negative going wave generated by a point excitation can be calculated by solving

$$\begin{bmatrix}\boldsymbol{\phi}_{\mathrm{q}}^+ & -\boldsymbol{\phi}_{\mathrm{q}}^- \\ \boldsymbol{\phi}_{\mathrm{f}}^+ & -\boldsymbol{\phi}_{\mathrm{f}}^-\end{bmatrix}\begin{Bmatrix}\mathbf{e}^+ \\ \mathbf{e}^-\end{Bmatrix} = \begin{Bmatrix}\mathbf{0} \\ \mathbf{f}_{ext}\end{Bmatrix}, \tag{10}$$

either by direct inversion or by using the orthogonality properties of the left eigenvector of the transfer matrix, for improved numerical conditioning [12,13]. The response to general excitation can be calculated following the procedure given by Renno and Mace [10]. A number of parameters yielding information about the wave propagation characteristics can be calculated from this approach. In this work, it is particularly interesting to calculate the time average power transmitted through the cross-section, i.e.

$$P = -\frac{1}{2}\mathrm{Re}\{i\omega\mathbf{f}^H\mathbf{q}\} = \frac{\omega}{2}\mathrm{Im}\{\mathbf{f}^H\mathbf{q}\}, \tag{11}$$

where the superscript H stands for the Hermitian.

4. Wave propagation with slowly varying properties

For the WKB approximation, it is necessary to calculate the phase change considering the locally defined wavenumber $k_j(x)$ as well as the amplitude change caused by the slowly varying waveguide properties. In this section, the WFE approach is used to estimate $k_j(x)$ at a number of points for calculating the phase change $\theta_j(x_a, x_b)$ from x_a to x_b. A numerical integration using a Gauss-Legendre quadrature scheme is applied, i.e.

$$\theta_j(x_a, x_b) = \int_{x_a}^{x_b} k_j(x)\,dx \approx \sum_{i=1}^{N_{gl}} G_i k_j(x_i), \tag{12}$$

where G_i are the weights and $k_j(x_i)$ is the j^{th} wavenumber calculated at the sampling point x_i defined from the Gauss-Legendre quadrature. The proprieties are evaluated at x_i from a given function describing the spatial variability and then assumed constant within the WFE cross-section. This is equivalent to a mid-point discretization for the spatial variability given by a random field, [21–23]. The integration scheme gives the exact integral for a polynomial of a given order depending on the number of points N_{gl}. Therefore, this is equivalent to a polynomial fitting of the wavenumber over the waveguide between x_a and x_b. The number of points used by the quadrature must be kept to a minimum number

of evaluations, to avoid excessive computational cost. No re-meshing of the FE model is necessary for each WFE evaluation.

The amplitude change can be calculated from the energy conserving property as a consequence of the WKB approximation [14,24]. Therefore, for a positive-going wave travelling from x_a, with amplitude a^+, to x_b, with amplitude b^+, as shown in Fig. 2, assuming no damping, the time average power transmitted through the cross-section, Eq. (11), at both positions must be equal, leading to

$$\left|a_j^+\right|^2 Re\left\{i\omega \boldsymbol{\Phi}_{f,j}^{+H}(x_a)\boldsymbol{\Phi}_{q,j}^{+}(x_a)\right\} = \left|b_j^+\right|^2 Re\left\{i\omega \boldsymbol{\Phi}_{f,j}^{+H}(x_b)\boldsymbol{\Phi}_{q,j}^{+}(x_b)\right\}. \tag{13}$$

This relation is written in order to define the amplitude change, giving

$$\gamma_j(x_a,x_b) = \log\left(\frac{|b^+|}{|a^+|}\right) = \frac{1}{2}\log\left(\frac{Re\left\{i\omega \boldsymbol{\Phi}_{f,j}^{H}(x_a)\boldsymbol{\Phi}_{q,j}(x_a)\right\}}{Re\left\{i\omega \boldsymbol{\Phi}_{f,j}^{H}(x_b)\boldsymbol{\Phi}_{q,j}(x_b)\right\}}\right). \tag{14}$$

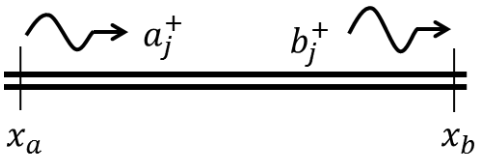

Figure 2. Positive-going wave travelling from x_a, with amplitude a_j^+, to x_b, with amplitude b_j^+, in an infinite waveguide.

5. Application example: straight beam

In this application example, an Euler-Bernoulli straight beam undergoing flexural vibration with propagating and evanescent waves is considered. The proposed finite element approach for wave propagation is applied for slowly varying material and geometrical properties, considering deterministic and random variability. A case of geometric non-uniformity to which analytical solutions are available [4] is also presented.

5.1. WKB and finite element approach

In the case of flexural vibration, the governing equation with spatially varying properties is given by

$$\frac{\partial^2}{\partial x^2}\left[EI(x)\frac{\partial^2 w(x,t)}{\partial x^2}\right] + \rho A(x)\frac{\partial^2 w(x,t)}{\partial t^2} = q(x,t), \tag{15}$$

where $EI(x)$ is the spatially varying bending stiffness, $\mathrm{q}(x,t)$ is the excitation per unit length and $w(x,t)$ is the flexural displacement. Assuming a time harmonic solution $w(x,t) = W(x)e^{-\mathrm{i}\omega t}$, thus the *eikonal* $S(x)$ is also used here in order to find wave solutions of the kind $W(x) = \widetilde{W}(x)e^{\pm \mathrm{i}\theta(x)}$. Propagating and evanescent waves are therefore taken into account, and then the propagation matrices are given by [15]

$$\boldsymbol{\Lambda}^+(x_a,x_b) = diag\{\exp[-\mathrm{i}\theta_B(x_a,x_b) + \gamma_B(x_a,x_b)], \exp[-\theta_B(x_a,x_b) + \gamma_B(x_a,x_b)]\}, \tag{16}$$

$$\boldsymbol{\Lambda}^-(x_a,x_b) = diag\{\exp[-i\theta_B(x_a,x_b) - \gamma_B(x_a,x_b)], \exp[-\theta_B(x_a,x_b) - \gamma_B(x_a,x_b)]\}, \tag{17}$$

where $diag\{\cdot\}$ stands for a diagonal matrix, and

$$\theta_B(x_a,x_b) = \int_{x_a}^{x_b} k_B(x)dx, \tag{18}$$

and for a wave propagating between two arbitrary points x_1 and x_2, with $k_B(x) = [\rho A(x)\omega^2 EI^{-1}(x)]^{1/4}$ as the local wavenumber of the flexural wave, and the amplitude change

$$\gamma_B(x_1, x_2) = \frac{1}{2}\ln\left[\frac{\widetilde{W}(x_2)}{\widetilde{W}(x_1)}\right], \tag{19}$$

where $\widetilde{W}(x) = [\rho A(x)]^{-\frac{3}{8}}\left[EI_{yy}(x)\right]^{-\frac{1}{8}}$ are the wave amplitudes [14].

A FE model for the beam cross-section is built using a single Euler-Bernoulli element with two nodes and two degree of freedom per node [25] assuming constant properties within the each element. The forced response requires a number N_{gl} of WFE evaluations for the calculation of propagation matrices at the left and N_{gl} at the right side of the excitation point, one evaluation at the left and right boundaries and one evaluation at the excitation point itself, with a total of $N_{eval} = 2N_{gl} + 3$ WFE evaluations. Figure 3 presents these evaluations for $N_{gl} = 3$ compared to the homogeneous case, in which only one WFE evaluation is necessary.

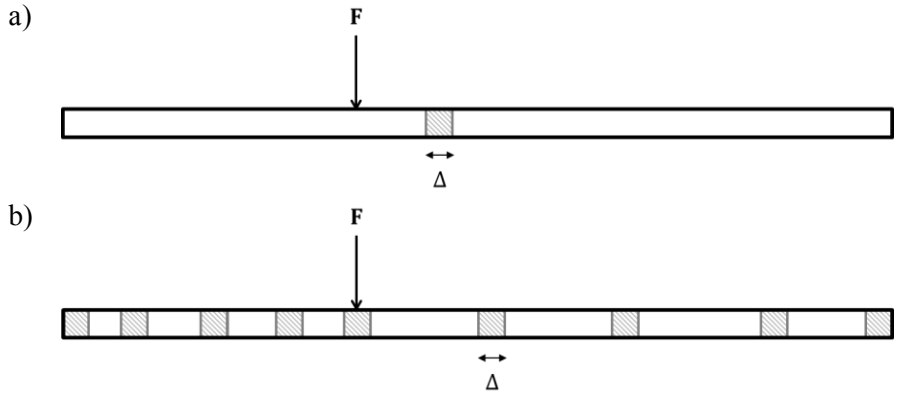

Figure 3. WFE evaluations for (a) homogeneous and (b) slowly varying waveguide for Gauss-Legendre integration of order 3.

5.2. Analytical solution for non-uniform cross-sectional area

Assuming that the material properties of beam are constant while the cross-sectional area and the second moment of area are given by $A(x) = \alpha_A x^\mu$ and $I(x) = \alpha_I x^{\mu+2}$, where $\alpha_A > 0$, $\alpha_I > 0$, $x > 0$ and $\mu \geq 0$ is the flaring index, then an analytical solution of Eq. (15) can be found in terms of a linear combination of Hankel and modified Bessel functions representing positive and negative going propagating and evanescent waves, such that [4]

$$W(x) = x^{\mu/2}\left[C_1 H_\mu^{(2)}(2k_B(x)x) + C_2 K_\mu(2k_B(x)x) + C_3 H_\mu^{(1)}(2k_B(x)x) + C_4 I_\mu(2k_B(x)x)\right], \tag{20}$$

where C_1, C_2, C_3, C_4 are arbitrary constants and $H_\mu^{(1,2)}(2k_B(x)x)$ is the Hankel function of the first and second kind, of order μ and argument $(2k_B(x)x)$ and $I_\mu(2k_B(x)x)$ and $K_\mu(2k_B(x)x)$ are the modified Bessel functions of the first and second kind of order μ Expressions for the displacement and internal forces matrices for positive and negative going waves are given by

$$\boldsymbol{\Phi}_q^+ = \begin{bmatrix} 1 & 1 \\ -k_B(x)\dfrac{H_{\mu+1}^{(2)}(2k_B(x)x)}{H_\mu^{(2)}(2k_B(x)x)} & k_B(x)\dfrac{K_{\mu+1}(2k_B(x)x)}{K_\mu(2k_B(x)x)} \end{bmatrix}, \tag{21}$$

$$\boldsymbol{\Phi}_q^- = \begin{bmatrix} 1 & 1 \\ -k_B(x)\dfrac{H_{\mu+1}^{(1)}(2k_B(x)x)}{H_\mu^{(1)}(2k_B(x)x)} & k_B(x)\dfrac{I_{\mu+1}(2k_B(x)x)}{I_\mu(2k_B(x)x)} \end{bmatrix}, \tag{22}$$

$$\boldsymbol{\Phi}_f^+ = \begin{bmatrix} -k_B^3(x)\dfrac{H_{\mu+1}^{(2)}(2k_B(x)x)}{H_\mu^{(2)}(2k_B(x)x)} & k_B^3(x)\dfrac{K_{\mu+1}(2k_B(x)x)}{K_\mu(2k_B(x)x)} \\ k_B^2(x)\dfrac{H_{\mu+2}^{(2)}(2k_B(x)x)}{H_\mu^{(2)}(2k_B(x)x)} & k_B^2(x)\dfrac{K_{\mu+2}(2k_B(x)x)}{K_\mu(2k_B(x)x)} \end{bmatrix}, \tag{23}$$

$$\boldsymbol{\Phi}_q^- = \begin{bmatrix} -k_B^3(x)\dfrac{H_{\mu+1}^{(1)}(2k_B(x)x)}{H_\mu^{(2)}(2k_B(x)x)} & -k_B^3(x)\dfrac{I_{\mu+1}(2k_B(x)x)}{I_\mu(2k_B(x)x)} \\ k_B^2(x)\dfrac{H_{\mu+2}^{(1)}(2k_B(x)x)}{H_\mu^{(2)}(2k_B(x)x)} & k_B^2(x)\dfrac{I_{\mu+2}(2k_B(x)x)}{I_\mu(2k_B(x)x)} \end{bmatrix}, \tag{24}$$

i.e. $\boldsymbol{\Phi}_q^+$, $\boldsymbol{\Phi}_q^-, \boldsymbol{\Phi}_f^+$ and $\boldsymbol{\Phi}_f^-$, can be found analytically in terms of these functions. The propagation matrices between x_a and x_b are given by

$$\boldsymbol{\Lambda}^+(x_a, x_b) = diag\left\{\left(\frac{x_a}{x_b}\right)^{\mu/2} \frac{H_\mu^{(2)}\left[2k_B(x_a)(x_a x_b)^{1/2}\right]}{H_\mu^{(2)}\left(2k_B(x_a)\right)}, \frac{K_\mu\left[2k_B(x_a)(x_a x_b)^{1/2}\right]}{K_\mu(2k_B(x_a)x_a)}\right\}, \tag{25}$$

$$\boldsymbol{\Lambda}^-(x_a, x_b) = diag\left\{\left(\frac{x_b}{x_a}\right)^{\mu/2} \frac{H_\mu^{(1)}(2k_B(x_a)x_a)}{H_\mu^{(1)}[2k_B(x_a)(x_a x_b)^{1/2}]}, \frac{I_\mu(2k_B(x_a)x_a)}{I_\mu[2k_B(x_a)(x_a x_b)^{1/2}]}\right\}. \tag{26}$$

The amplitudes of the positive and negative going waves generated by a point excitation at $x = L_e$ are identical and are given by

$$\mathbf{e}^\pm = -\frac{f_{ext}L_e}{4EI(L_e)k_B^2(L_e)} \begin{Bmatrix} i\pi \left|H_\mu^{(2)}(2k_B(x_a)x_a)\right| \\ 4K_\mu(2k_B(x_a)x_a)I_\mu(2k_B(x_a)x_a) \end{Bmatrix}, \tag{27}$$

Moreover, reflection matrices can be found by using Eq. (9), and the forced response can be calculated from Eqs. (3) and (4). More details on this formulation can be found in [4].

6. Random variability

Random field theory can be used to model spatially distributed randomness using a probability measure. There are a number of methods available in the literature for generating random fields [22,23,26,27], including formulations using series expansions that are able to represent the field using deterministic spatial functions and random uncorrelated variables. The KL expansion is a special case where these deterministic spatial functions are orthogonal and derived from the covariance function.

A Gaussian homogeneous random field $H(x,p)$ with a finite, symmetric and positive definite covariance function $C_H(x_1,x_2)$, defined over a domain D, has a spectral decomposition in a generalized series as [26]

$$H(x) = H_0(x) + \sum_{j=1}^{\infty} \sqrt{\lambda_j}\,\xi_j f_j(x), \tag{28}$$

where ξ_j are Gaussian uncorrelated random variables, λ_j and $f_j(x)$ are eigenvalues and eigenfunctions. The eigenvalues and eigenfunctions can be ordered in descending order of eigenvalues and the KL expansion is then calculated with a finite number of terms N_{KL}, chosen by the accuracy of the series in representing the covariance function [28]. As a rule of thumb, N_{KL} can be chosen such that $\lambda_{N_{KL}}/\lambda_1 < 0.1$, and N_{KL} will depend on the correlation length of the random field.

In general, this problem can only be solved numerically by discretizing the covariance function. However, for some families of correlation functions and specific geometries, there exist analytical solutions. One such case is the one dimensional exponentially decaying autocorrelation function, $C(x_1,x_2) = e^{-|x_1-x_2|/l_c}$, where l_c is the correlation length, in the interval $-L/2 \le x \le L/2$, where L is the length of the domain and where x_1 and x_2 are any two points within the interval. In this case, the KL expansion, for a zero-mean random field, can be written as

$$H(x) = \sum_{j=1}^{N_{kl}} \left[\alpha_j \xi_{1j} \sin(w_{1j}x) + \beta_j \xi_{2j} \cos(w_{2j}x)\right] \tag{29}$$

where ξ_{1j} and ξ_{2j} are Gaussian zero-mean, unity standard-deviation, independent random variables with the properties $\langle\xi_{1j}\rangle = \langle\xi_{1i}\rangle = 0, \langle\xi_{1i}\xi_{2j}\rangle = 0\,, \langle\xi_{1i}\xi_{1j}\rangle = \delta_{ij}$ where $\delta_{ij} = 1$ for $i = j$ and $\delta_{ij} = 0$ for $i \neq j$, and $\alpha_j = \sqrt{\lambda_{1j}/\left(\frac{L}{2} - \frac{\sin(w_{1j}L)}{2w_{1j}}\right)}$, $\beta_j = \sqrt{\lambda_{2j}/\left(\frac{L}{2} + \frac{\sin(w_{2j}L)}{2w_{2j}}\right)}$, $\lambda_{1j} = 2c/\left(w_{1i}^2 + c^2\right)$, $\lambda_{2j} = 2c/\left(w_{2i}^2 + c^2\right)$, where $c = 1/b$ and w_{1i} and w_{2i} are the i^{th} roots of the transcendental equations $c\tan w_1 + w_1 = 0$ and $w_2 \tan w_2 - c = 0$, respectively. This expansion is truncated to N_{KL} terms according the weight of the higher order eigenvalues in the series. A complete derivation can be found in the book by Ghanem and Spanos [26].

The KL expansion is then used to describe the Young's modulus as a random field in the numerical examples of the following section, given by $E(x) = E_0[1 + \sigma H(x)]$, where E_0 is the nominal value for the Young's modulus and σ is the standard deviation, that can also be seen as a dispersion term quantifying the influence of $H(x)$ on the mean value E_0. The slowly varying condition can be achieved by choosing an appropriate value of the correlation length b. The larger the correlation length, the smoother the spatial variability. The Gaussian probability distribution implies that the Young's modulus could assume negative values, but the choice of the parameters makes it a very unlikely event. From a Monte Carlo (MC) sampling framework, the distribution can be clipped to avoid values of Young`s modulus smaller than a given threshold. Even though an analytical solution of the KL expansion is used in this work, the proposed method is not restricted to it and any numerical solution for a different correlation function or probability density function can be applied.

7. Numerical examples

In this section, two numerical examples are presented. The first considers a deterministic non-uniform cross-sectional area, such that analytical solutions are available, as shown in section 5.2. The second considers deterministic and stochastic material variability. Specifically, the Young's modulus is modelled as a Gaussian random field with an autocorrelation function such that Eq. (29) can be used. The deterministic material variability considers a single sample from the random field to generate a spatially varying Young's modulus. The statistics of the response for the stochastic analysis are calculated from a MC scheme with 2000 samples.

Both examples use an aluminium beam undergoing flexural vibration with spatially varying Young's modulus and constant mass density $\rho = 2700$ kg/m^3, with $L = 1$ m total length, free-free boundary conditions and point excitation at $L_e = 0.15L$. The phase change $\theta(x_a, x_b)$ for the propagation matrices $\mathbf{\Lambda}^+(x_a, x_b)$, Eq.(16), and $\mathbf{\Lambda}^-(x_a, x_b)$, Eq. (17), was calculated from the wavenumbers found in the WFE analysis with a segment length $\Delta = 0.01$ m, Eq. (12), evaluated with $N_{gl} = 3$, for the first example, and $N_{gl} = 5$ points, for the second example, defined by the Gauss-Legendre quadrature scheme over the waveguide and assuming constant properties within the segment. For calculation of the forced response a total of $N_{eval} = 2N_{gl} + 3 = 9$ and $N_{eval} = 2N_{gl} + 3 = 13$ WFE evaluations were needed for the first and second example, respectively. This procedure was repeated for each MC sample. A standard FE model was used for comparison with 150 elements and mid-point random field discretization.

In the first case, the section is assumed rectangular with constant width $b = 50$ mm and linearly changing height, i.e. $\mu = 1$, with height $h_L = 1$ mm at the left boundary and $h_R = 3$ mm at the right boundary, i.e. a three times increase, and Young's modulus $E = 70$ GPa. Structural damping is included using a complex Young's modulus $E(1 + i\eta)$, with $\eta = 10^{-3}$. Figure 4 shows the wavenumber divided by $\omega^{1/2}$ along the beam obtained with the analytical solution and with the WFE evaluations. Note that both approaches present a very good agreement and for an increasing height there is a decreasing wavenumber, because $k_B(x) \propto h^{-1/2}(x)$. Figure 5 presents the input mobility at $x = 0.15L$ using the standard FE, the analytical solution and the numerical WKB method. There is a good agreement for all the approaches.

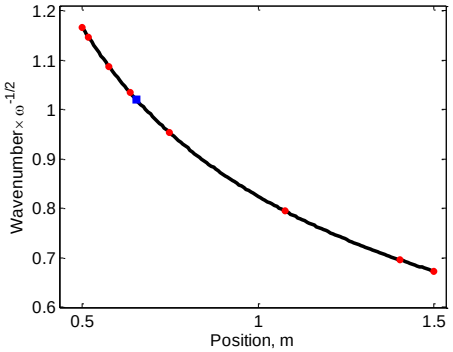

Figure 4. Normalized wavenumber along the beam with non-uniform linearly varying area using the analytical solution (black line) and the WFE (red circle), with $\mu = 1$ and $\Delta = 0.01$.

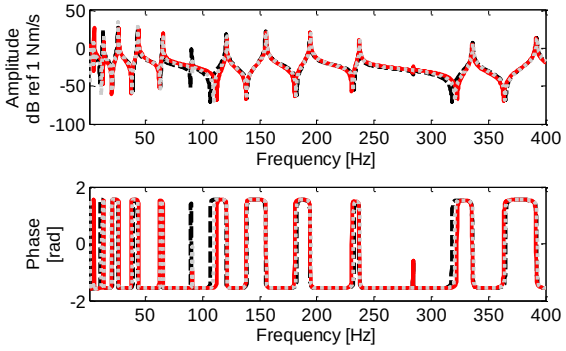

Figure 5. Input mobility at $x = 0.15L$ using FE (red), analytical (black dashed) and numerical WKB (grey dotted) for $\Delta = 0.01$ m.

In the second case, the Young's modulus is considered varying while the mass density and the geometric properties remain constant, with height $h = 1$mm. The nominal Young's modulus value is $E_0 = 70$ GPa and the random field has a standard deviation $\sigma = 0.1$ and correlation length $l_c = 0.1L$, which is ten times larger than Δ for the WFE analysis, and 15 times larger than the element size for the standard FE approach. Figure 6 presents a sample of the random field, normalized by the nominal value, along with the excitation point and the points used for integration using GL quadrature. Figure 7 shows

the input mobility at $x = 0.15L$ using the standard FE, the analytical and the numerical WKB approaches. A very good agreement can be found between both WKB approaches, numerical and using the WFE method.

Figure 8 shows input mobility 95% confidence bounds of the stochastic beam. It can be noticed that results from the WKB approach using numerical evaluation agree very well with the results from the analytical WKB and standard FE method.

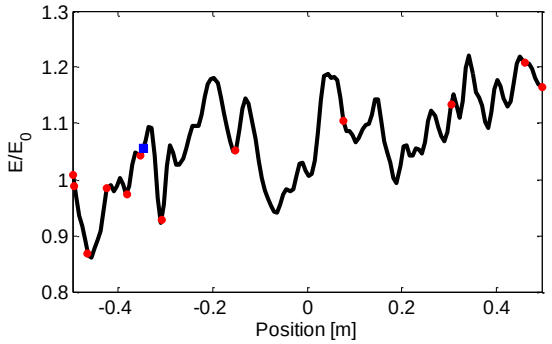

Figure 6. The Young's modulus as a function of the position used for the deterministic analysis, the WFE evaluation points (red dot) and excitation point (blue square).

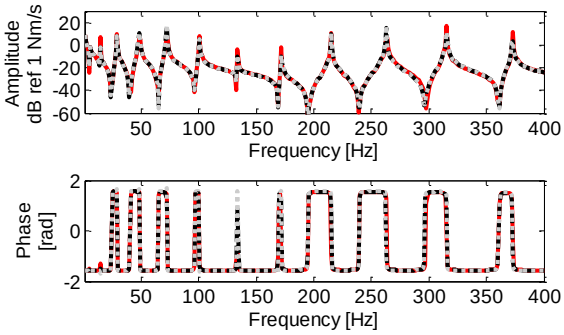

Figure 7. Input mobility at $x = 0.15L$ using FE (red), analytical WKB (black dashed) and numerical WKB (grey dotted) for $\Delta = 0.01$ m.

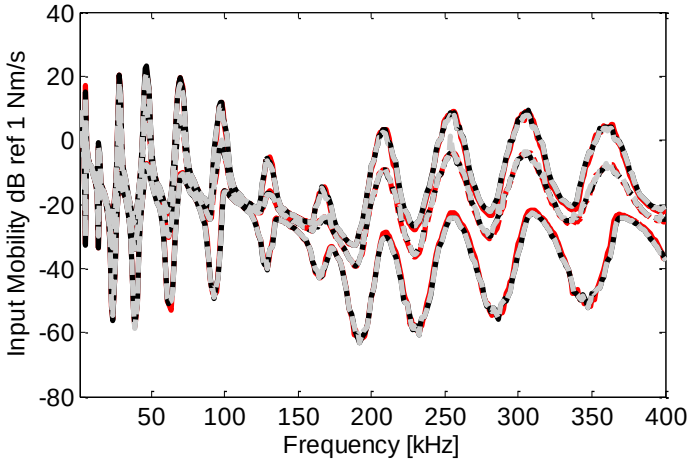

Figure 8. Input mobility 95% confidence bounds (full line) and mean value (dashed line) at $x = 0.15L$ using FE (red), analytical WKB (black) and numerical WKB (grey) with $\Delta = 0.01$ m using $\sigma = 0.1$ and $b = 0.25L$.

8. Concluding remarks

A method is proposed to extend the applicability of the WKB approach to cases where no analytical solution exists by using a FE approximation. The phase change requires the numerical evaluation of the locally defined wavenumber at various points, which are kept to a minimum, and is evaluated at locations defined by a Gauss-Legendre quadrature scheme. Also, the WKB solution implies conservation of power which is used to calculate the amplitude change.

An example of a straight beam undergoing flexural vibration is presented for two cases. In the first, a deterministic non-uniform cross-sectional area with shape such that analytical solutions are available, in terms of Hankel and modified Bessel functions. In the second, the spatially correlated random variability of the Young's modulus is expressed by a specific analytical solution of the KL expansion for random fields. Even though an analytical KL expansion is used, the method can be extended straightforwardly to a numerical solution of the KL expansion and therefore to different correlation

functions or probability density functions. Results are compared to a standard FE approach, using a mid-point random field discretization, and to the available analytical solution for the first case, and a good agreement is seen for all approaches. For the second case, results are compared with the analytical WKB approach and very good agreement is found within the validity of the WFE approximation, i.e. it depends on the FE discretization of the waveguide cross-section.

Further steps include extending the proposed approach to more complex waveguides, with different wave modes, exploring other random field types and the sensitivity to the random field discretization.

Acknowledgments
The authors gratefully acknowledge the financial support of the Brazilian National Council of Research (CNPq) Process number 445773/2014-6, the Federal District Research Foundation (FAPDF) Process number 0193001040/2015 and the Royal Society for the Newton International Exchanges Fund.

References

[1] Li Q S 2000 Exact solutions for free longitudinal vibrations of non-uniform rods *J. Sound Vib.* **234** 1–19
[2] Eisenberger M 1991 Exact longitudinal vibration frequencies of a variable cross-section rod *Appl. Acoust.* **34** 123–30
[3] Guo S and Yang S 2012 Wave motions in non-uniform one-dimensional waveguides *J. Vib. Control* **18** 92–100
[4] Lee S K, Mace B R and Brennan M J 2007 Wave propagation, reflection and transmission in non-uniform one-dimensional waveguides *J. Sound Vib.* **304** 31–49
[5] Ichchou M N, Akrout S and Mencik J M 2007 Guided waves group and energy velocities via finite elements *J. Sound Vib.* **305** 931–44
[6] Mace B R, Duhamel D, Brennan M J and Hinke L 2005 Finite element prediction of wave motion in structural waveguides *J. Acoust. Soc. Am.* **117** 2835–43
[7] Manconi E and Mace B R 2009 Wave characterization of cylindrical and curved panels using a finite element method *J. Acoust. Soc. Am.* **125** 154–63
[8] Mencik J-M 2014 New advances in the forced response computation of periodic structures using the wave finite element (WFE) method *Comput. Mech.* **54** 789–801
[9] Mencik J-M and Ichchou M N 2005 Multi-mode propagation and diffusion in structures through finite elements *Eur. J. Mech. - ASolids* **24** 877–98
[10] Renno J M and Mace B R 2010 On the forced response of waveguides using the wave and finite element method *J. Sound Vib.* **329** 5474–88
[11] Renno J M and Mace B R 2013 Calculation of reflection and transmission coefficients of joints using a hybrid finite element/wave and finite element approach *J. Sound Vib.* **332** 2149–64
[12] Waki Y, Mace B R and Brennan M J 2009 Numerical issues concerning the wave and finite element method for free and forced vibrations of waveguides *J. Sound Vib.* **327** 92–108
[13] Waki Y, Mace B R and Brennan M J 2009 Free and forced vibrations of a tyre using a wave/finite element approach *J. Sound Vib.* **323** 737–56
[14] Pierce A D 1970 Physical interpretation of the WKB or eikonal approximation for waves and vibrations in inhomogeneous beams and plates *J. Acoust. Soc. Am.* **48** 275–84
[15] Fabro A T, Ferguson N S, Jain T, Halkyard R and Mace B R 2015 Wave propagation in one-dimensional waveguides with slowly varying random spatially correlated variability *J. Sound Vib.* **343** 20–48
[16] Rienstra S W 2003 Sound propagation in slowly varying lined flow ducts of arbitrary cross-section *J. Fluid Mech.* **495** 157–73
[17] Arenas J P and Crocker M J 2001 A note on a WKB application to a duct of varying cross-section *Appl. Math. Lett.* **14** 667–71

[18] Firouz-Abadi R D, Haddadpour H and Novinzadeh A B 2007 An asymptotic solution to transverse free vibrations of variable-section beams *J. Sound Vib.* **304** 530–40
[19] Nayfeh A H 1973 *Perturbation methods* (New York: Wiley)
[20] Whitham G B 1974 *Linear and nonlinear waves* (New York: John Wiley & Sons)
[21] Der Kiureghian A and Ke J-B 1988 The stochastic finite element method in structural reliability *Probabilistic Eng. Mech.* **3** 83–91
[22] Stefanou G 2009 The stochastic finite element method: Past, present and future *Comput. Methods Appl. Mech. Eng.* **198** 1031–51
[23] Sudret B and Der Kiuereghian A 2000 *Stochastic Finite Element methods and reliability: A state-of-Art report* (University of California, Berkeley)
[24] Nielsen R and Sorokin S 2014 The WKB approximation for analysis of wave propagation in curved rods of slowly varying diameter *Proc R Soc A* **470** 20130718
[25] Petyt M 2010 *Introduction to Finite Element vibration analysis* (New York, USA: Cambridge University Press)
[26] Ghanem R and Spanos P D 2012 *Stochastic Finite Elements: A Spectral Approach* (Minneola, N.Y.: Dover Publications)
[27] Vanmarcke E 2010 *Random Field: Analysis and Synthesis* (Cambridge, MA: Word Scientific)
[28] Huang S P, Quek S T and Phoon K K 2001 Convergence study of the truncated Karhunen–Loeve expansion for simulation of stochastic processes *Int. J. Numer. Methods Eng.* **52** 1029–43